Synthesis, characterization, and application of CoFe$_2$O$_4$@TRIS@sulfated boric acid nanocatalyst for the synthesis of 2-amino-3-cyanopyridine derivatives

Homayoun Faroughi Niya[1] · Nourallah Hazeri[1] · Malek Taher Maghsoodlou[1] · Maryam Fatahpour[1]

Abstract
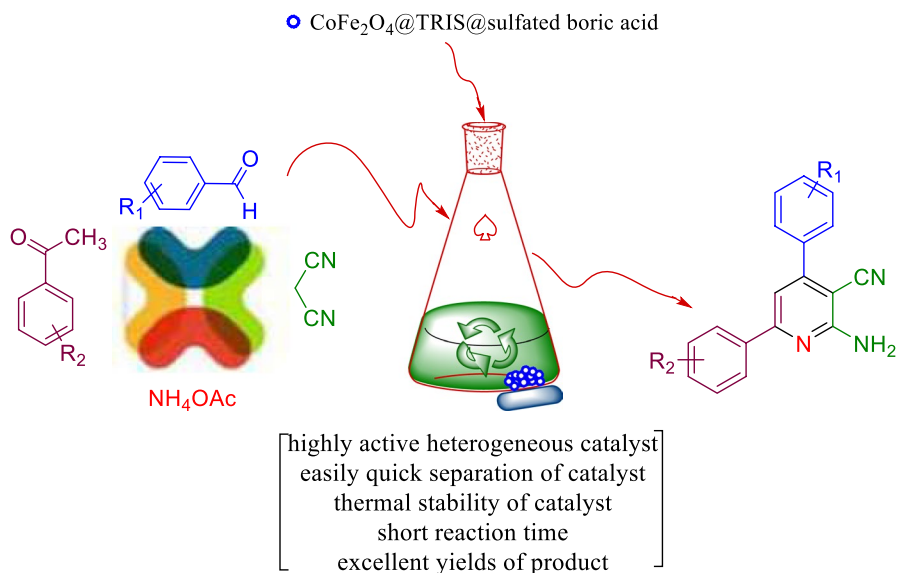
The aim of this research is the synthesis of a novel acidic nanocatalyst using the layer-by-layer assembly technique. The CoFe$_2$O$_4$@TRIS@sulfated boric acid nanoparticles were easily synthesized and studied as a highly beneficial, recyclable, and magnetite nanocatalyst for the synthesis of 2-amino-3-cyanopyridine derivatives. The chemical structure of CoFe$_2$O$_4$@TRIS @sulfated boric acid nanocatalyst was completely confirmed with different techniques like FESEM, Map, EDS, XRD, TGA/DTG, VSM, and FT-IR analyses. Briefly, the newly synthesized nanocatalyst offers some advantages such as simplicity of work-up, highly stable, environmental friendliness, reusability, excellent yields, and short reaction time.

✉ Nourallah Hazeri
  n_hazeri@yahoo.com; nhazeri@chem.usb.ac.ir

1 Department of Chemistry, Faculty of Science, University of Sistan and Baluchestan, P.O. Box 98135-674, Zahedan, Iran

Graphic abstract

$CoFe_2O_4$@TRIS@sulfated boric acid

highly active heterogeneous catalyst
easily quick separation of catalyst
thermal stability of catalyst
short reaction time
excellent yields of product

Keywords $CoFe_2O_4$@TRIS@sulfated boric acid · 2-Amino-3-cyanopyridine derivatives · Magnetite nanocatalyst · Reusable catalyst

Introduction

The progress of the research on magnetic nanomaterials (MNPs) has opened a novel perspective in the development of various areas of science such as biomedicine, magnetic resonance imaging, environmental remediation, catalysis, and high-density magnetic storage [1–4]. Magnetically separation of materials is a rapid and easy path for separation and recovery of catalysts from the reaction system. Over the past several decades, iron oxide (Fe_3O_4) MNPs have been widely reported as attractive candidates for the manufacture of supported solid catalysts. In this regard, bimetal oxide magnetic MNPs MFe_2O_4 (M: Co, Fe, Ni, Zn, Cu, and Mn) have been extremely studied owing to their meaningful applications. They allow a better tuning of the nanomaterials' properties (morphology, size, and monodispersion). Cobalt ferrites ($CoFe_2O_4$) MNPs have been demonstrated to be one of the most versatile magnetic systems due to their high saturation magnetization, large surface area-to-volume ratio, strong anisotropy, high coercivity and high mechanical hardness, chemical, and thermal stability [5, 6]. Nowadays, various magnetic nanocatalysts were prepared for the use in modern synthetic organic chemistry including 6-APA/γ-Fe_2O_3@SiO_2 [7], DDBSA@MNP [8], $CoFe_2O_4$@Pr [9], $CoFe_2O_4$@HT@Imine-CuII [10], Fe_3O_4@SiO_2-EDTA-Pd [11].

On the other hand, a growing interest has been shown on the production of functionalized magnetic nanoparticles for widespread applications as catalysis over conventional materials especially for the binding of homogeneous organocatalysts. The coated homogeneous catalysts on solid supports can be used to design the novel heterogeneous catalyst systems which have high catalytic activity and high surface area to increase catalyst coating along with simple separation from the reaction mixture [12].

Cyanopyridine derivatives are very well known for their wide range of biological properties such as antitumor [13], antibacterial [14], anti-cardiovascular [15], anti-inflammatory, analgesic, antipyretic [16], IKK-β inhibitors [17], potent inhibitor of HIV-1 integrase [18], and A2A adenosine receptor antagonists [19].

Considering all the aforementioned points and in continuation of our research to develop the synthesis of new solid acid catalyst systems for the important organic conversions [20–23], herein, we have been successfully immobilized TRIS@sulfated boric acid onto $CoFe_2O_4$ nanostructured and further applied as a novel efficient, and reusable nanocatalyst with excellent catalytic activity for a one-pot four-component synthesis of 2-amino-3-cyanopyridine from the reaction between aryl aldehydes **1**, malononitrile **2**, ketones **3**, and ammonium acetate **4** (Scheme 1). It is noteworthy that this is the first report on the synthesis of $CoFe_2O_4$@TRIS@sulfated boric acid magnetic nanoparticles that can be reused up to five times without notable reduction in its catalytic activity.

Experimental

General

Melting points of pure products were obtained using an Electrothermal melting point apparatus (type 9100). All applied chemicals were prepared from Merck and Aldrich companies in high purity. BRUKER DRX 300 MHz in DMSO at 300 Hz and FT-IR-JASCO-460 plus spectrometer were applied to record ^{1}H NMR and FT-IR spectras related to known compounds, respectively.
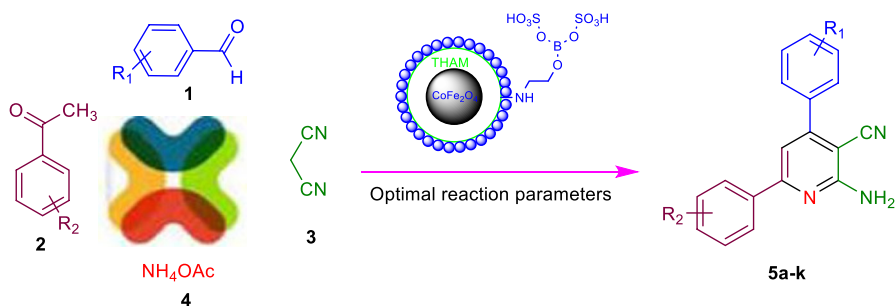
Scheme 1 The synthesis of 2-amino-3-cyanopyridine derivatives in the presence of novel acidic nanocatalyst

Synthesis of the magnetic CoFe$_2$O$_4$ nanoparticles

The KOH solution (1.0 M) was slowly added to 100 mL of an aqueous solution containing 1.0 mmol of CoCl$_2$·6H$_2$O and 2.0 mmol of FeCl$_3$·6H$_2$O until the pH of 11–12 was reached. Thereafter, the prepared solution was refluxed for 3 h at 140 °C under N$_2$ atmosphere and vigorous stirring at 1000 rpm. Lastly, the synthesized CoFe$_2$O$_4$ nanoparticles (black precipitate) were magnetically collected and purified several times using ethanol and water and dried at 60 °C.

Synthesis of the magnetic CoFe$_2$O$_4$@TRIS nanoparticles

CoFe$_2$O$_4$@TRIS nanoparticles were synthesized by a simple method. Initially, a known amount (0.2 g) of the CoFe$_2$O$_4$ MNPs was dispersed in 20 mL of ethanol using an ultrasonic bath for 15 min. Then, 0.4 g of tris (hydroxymethyl) aminomethane (TRIS, trisamine) was added to the magnetic solution and the resulting mixture was refluxed under N$_2$ atmosphere for 24 h at 100 °C. Finally, the obtained CoFe$_2$O$_4$@TRIS MNPs were separated, washed, and dried at 60 °C for 8 h.

Synthesis of the magnetic CoFe$_2$O$_4$@TRIS–CH$_2$CH$_2$–Cl nanoparticles

0.05 mL of triethylamine and 0.5 mL of dichloroethane were added dropwise to the mixture of the dispersed CoFe$_2$O$_4$@TRIS nanoparticles (0.2 g) in acetonitrile (20 mL). Then, the resulting mixture was refluxed under N$_2$ atmosphere for 24 h at 90 °C. Finally, the obtained CoFe$_2$O$_4$@TRIS–CH$_2$CH$_2$–Cl MNPs were separated, washed, and dried at 60 °C for 8 h.

Synthesis of magnetite CoFe$_2$O$_4$@TRIS@boric acid nanoparticles

Initially, 0.5 g of boric acid was added to the mixture of the dispersed CoFe$_2$O$_4$@TRIS–CH$_2$CH$_2$–Cl (0.2 g) in dry toluene (5 mL). Thereafter, the resulting mixture was refluxed for 1 day under N$_2$ atmosphere. Lastly, the achieved CoFe$_2$O$_4$@TRIS@boric acid nanoparticles were magnetically collected and purified several times using ethanol and water and dried at 60 °C.

Synthesis of magnetite CoFe$_2$O$_4$@TRIS@sulfated boric acid nanoparticles

Firstly, 0.2 g of CoFe$_2$O$_4$@TRIS@boric acid nanoparticles were ultrasonically dispersed in 5 mL of dry toluene. Next, chlorosulfonic acid (0.5 mL) was added dropwise and stirred at room temperature for 3 h. Afterward, the synthesized

CoFe$_2$O$_4$@TRIS@sulfated boric acid MNPs were magnetically collected and purified several times using ethanol and water, lastly dried at 80 °C.

General procedure for the four-component synthesis of 2-amino-3-cyanopyridine derivatives

CoFe$_2$O$_4$@TRIS@sulfated boric acid nanocatalyst (0.01 g) was entered into a vial containing a mixture of acetophenone derivatives (1.0 mmol), malononitrile (1.0 mmol), ammonium acetate (1.5 mmol) as a nitrogen source, and aromatic aldehydes (1.0 mmol). The final mixture was placed at 90 °C in an oil bath for a certain time and the reaction was followed by TLC. After completing the reaction, the mixture was cooled to room temperature. The resulting solid product was dissolved in hot ethanol, and then the CoFe$_2$O$_4$@TRIS@sulfated boric acid nanocatalyst was conveniently removed from the solution by an external magnet. Finally, the resulting solution was cooled to room temperature to the crude product was crystallized to afford the pure products.

Selected spectra for five Known products are given below

2-Amino-4,6-bis(4-chlorophenyl)nicotinonitrile (5a))

FT-IR (KBr): ν 822, (C–H), 1581, 1609 (C=C), 2206 (CN), 2922 (CH$_{aliphatic}$), 3461, 3501 (NH$_2$). ^{1}H-NMR (300 MHz, DMSO-d6): (δ, ppm): 8.18 (d, 2H, Ar–H) 7.56–7.74 (m, 6H, Ar–H), 7.33 (s, 1H, Ar–H), 7.12 (s, 2H, NH$_2$).

2-Amino-4,6-diphenylnicotinonitrile (5b)

FT-IR (KBr): ν 685, 753, (C–H), 1592, 1516 (C=C), 2198 (CN), 2956, 2919 (CH$_{aliphatic}$), 3063 (CH$_{aromatic}$), 3471, 3324 (NH). ^{1}H-NMR (300 MHz, DMSO-d6): (δ, ppm): 7.50–8.17 (m, 10H, Ar–H), 7.30 (s, 1H, Ar–H), 7.05 (s, 2H, NH$_2$).

2-Amino-6-(4-chlorophenyl)-4-(3,4-dimethoxyphenyl)nicotinonitrile (5c)

FT-IR (KBr): ν 762, 808 (C–H), 1554, 1516 (C=C), 2205 (CN), 2956, 2997 (CH$_{aliphatic}$), 3225 (CH$_{aromatic}$), 3369, 3496 (NH). ^{1}H-NMR (300 MHz, DMSO-d6): (δ, ppm): 8.19 (d, $J = 8.1$, 2H, Ar–H), 7.58 (d, $J = 8.4$, 2H, Ar–H), 7.13–7.34 (m, 4H, Ar–H), 7.02 (s, 2H, NH$_2$), 3.87 (s, 3H, OCH$_3$), 3.86 (s, 3H, OCH$_3$).

2-Amino-6-(4-chlorophenyl)-4-(3-nitrophenyl)nicotinonitrile (5d)

FT-IR (KBr): ν 811, 826, 743 (C–H), 1533, 1622 (C=C), 2204 (CN), 3090 (C–H$_{aromatic}$), 3398, 3498 (NH). ^{1}H-NMR (300 MHz, DMSO-d6): (δ, ppm): 8.54 (s, 1H, Ar–H), 8.41 (d, $J = 7.2$, 1H, Ar–H), 8.20 (m, 3H, Ar–H), 7.88 (t, J = 7.2, 1H, Ar–H), 7.59 (d, $J = 7.5$, 2H, Ar–H), 7.47 (s, 1H, Ar–H), 7.22 (s, 2H, NH$_2$).

2-Amino-4-(4-chlorophenyl)-6-phenyl nicotinonitrile (**5e**)

FT-IR (KBr): ν 687, 770, 826 (C–H), 1546, 1574 (C=C), 2216 (CN), 3361, 3484 (NH). ^{1}H-NMR (300 MHz, DMSO-d6): (δ, ppm): 8.15 (dd, 2H, Ar–H), 7.49–7.75 (m, 7H, Ar–H), 7.31 (s, 1H, Ar–H), 7.09 (s, 2H, NH$_2$).

Results and discussion

Synthesis and characterization of catalyst

The novel nanocatalyst (CoFe$_2$O$_4$@TRIS@sulfated boric acid) was synthesized based on the stages shown in Scheme 2. As can be seen, the chlorosulfonic acid was immobilized on the surface of CoFe$_2$O$_4$ magnetic nanoparticles using trisamine, dichloroethane, and boric acid.

The synthesized CoFe$_2$O$_4$@TRIS@sulfated boric acid nanocatalyst was characterized by scanning electron microscopy (SEM), X-ray mapping, energy-dispersive X-ray spectroscopy (EDS), Fourier transform infrared (FT-IR), differential thermal analysis (DTA), thermal gravimetric analysis (TGA), X-ray Diffraction (XRD), and vibrating sample magnetometer (VSM) techniques.

To confirm the structure of CoFe$_2$O$_4$@TRIS@sulfated boric acid nanoparticles, FT-IR spectroscopy was initially studied. The typical FT-IR spectra of CoFe$_2$O$_4$ (**a**), and CoFe$_2$O$_4$@TRIS@sulfated boric acid (**b**) are shown in Fig. 1. The adsorption peak at 618 cm^{-1} can be assigned to the Fe–O and Co–O in CoFe$_2$O$_4$ MNPs which shifts to 593 cm^{-1} after coating with the organic layer (Fig. 1a, b). Also, an intense absorption band at 3373 cm^{-1} is related to Co–OH stretching vibration. Furthermore, the peaks which appeared at 1044–1215 cm^{-1} correspond to the O=S=O symmetric
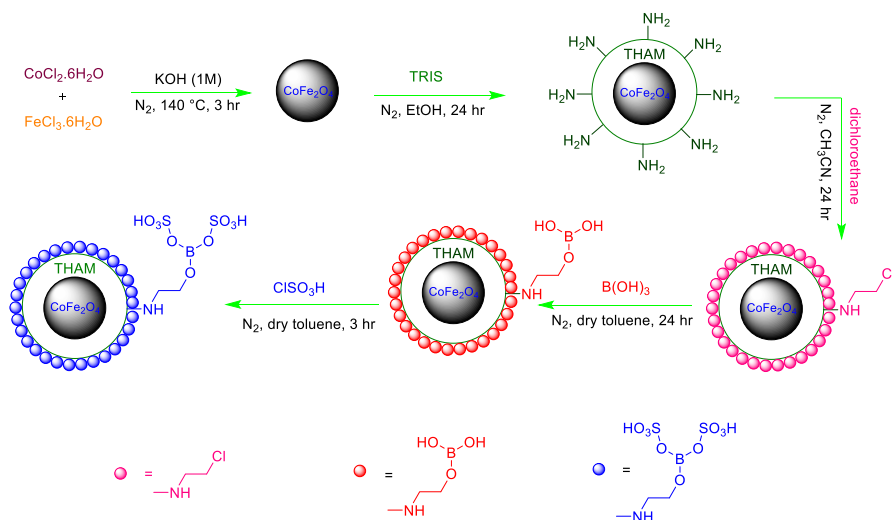
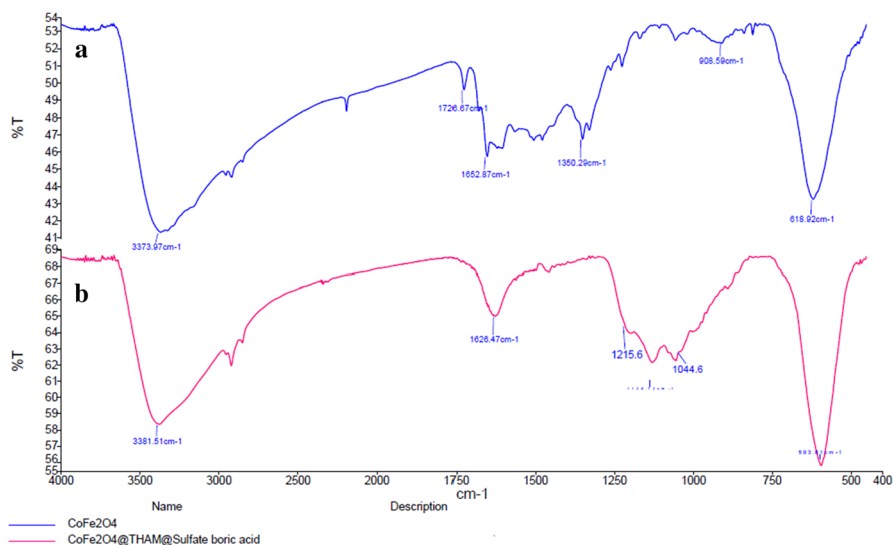**Scheme 2** Synthetic pathway for construction of CoFe$_2$O$_4$@TRIS@sulfated boric acid nanocatalyst

Fig. 1 FT-IR spectra of $CoFe_2O_4$ (**a**) and $CoFe_2O_4$@TRIS@sulfated boric acid (**b**) MNPs

and asymmetric stretching modes of $-SO_3H$ groups on the $CoFe_2O_4$@TRIS@sulfated boric acid surface (Fig. 1b). Additionally, the FT-IR spectrum of $CoFe_2O_4$@TRIS@sulfated boric acid MNPs (Fig. 1b) indicates two bands at 1626 cm^{-1} and 2923 cm^{-1} that are clear evidence for existing of the surface-adsorbed water and the C–H stretching vibrations in the aliphatic groups, respectively.

To earn further data about the synthesized nanoparticles, the morphology, and size of $CoFe_2O_4$, and $CoFe_2O_4$@TRIS@sulfated boric acid MNPs were investigated by the FESEM method. As depicted in Fig. 2, both images (Fig. a, a1, b, b1) show that the prepared nanoparticles have a nearly spherical shape. Moreover, the $CoFe_2O_4$@TRIS@sulfated boric acid MNPs (Fig. 3) have the same sizes (19.20 nm) in comparison with $CoFe_2O_4$ (19.46 nm). Therefore, it can be concluded that the organic layer coating onto the $CoFe_2O_4$ MNPs (TRIS@sulfated boric acid) has no effect on the morphology and the size of $CoFe_2O_4$ MNPs.

EDS and X-ray mapping techniques were also applied as two practical methods for generating qualitative data on the distribution of various elemental compositions in the nanocatalyst (Figs. 4, 5). The EDS spectrum of the $CoFe_2O_4$@TRIS@sulfated boric acid MNPs showed the content of nitrogen (N, 2.74%), carbon (C, 7.71%), boron (B, 11.84%), oxygen (O, 37.44%), and sulfur (S, 1.38%) signal peaks, which confirms $CoFe_2O_4$@TRIS@sulfated boric acid MNPs were successfully synthesized (Fig. 4). Furthermore, Fig. 5 shows the elemental map of the nanocatalyst. As can be seen, the elements of C, N, B, and S are homogeneously distributed and they are distinguishable in the prepared sample. These results confirm the EDS results (Fig. 5).

TGA technique was used to evaluate the thermal stability of $CoFe_2O_4$@TRIS@sulfated boric acid nanoparticles. As shown in Fig. 6, the TGA curve of $CoFe_2O_4$@TRIS@sulfated boric acid showed three steps of mass loss following the rise in temperature. The first one, in the regions 25–150 °C (about 2.54%)
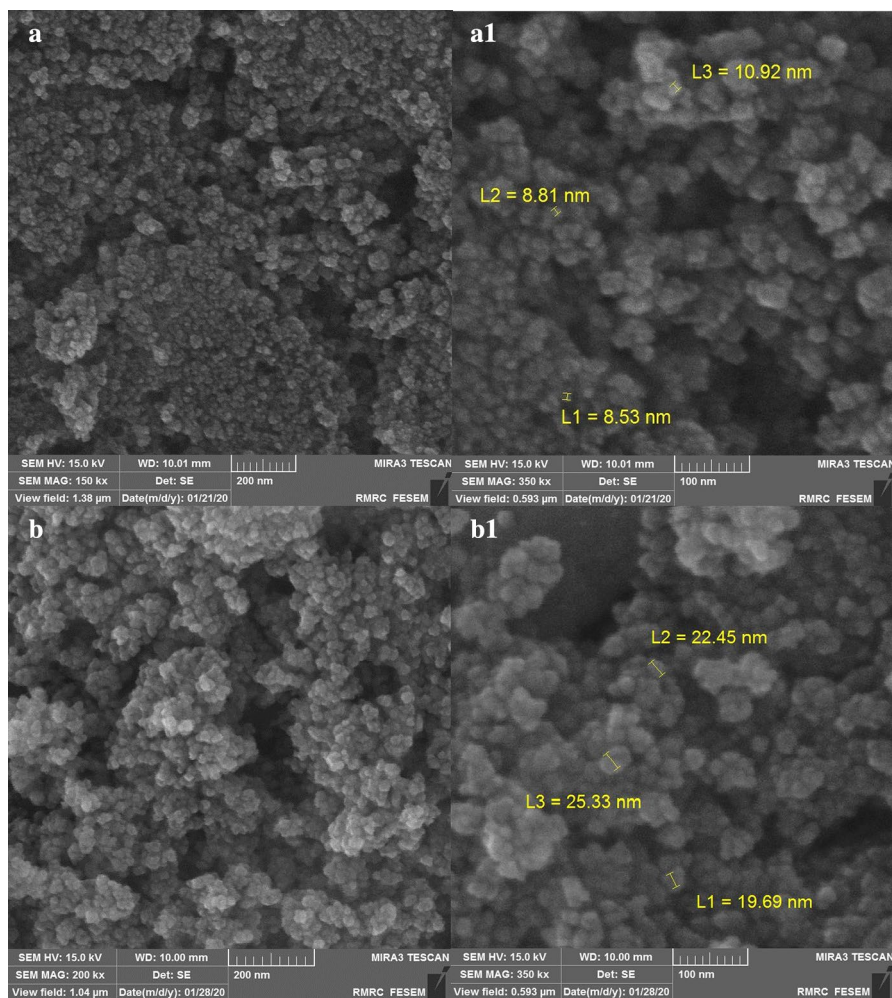
Fig. 2 FESEM images of $CoFe_2O_4$ (**a**, **a1**) and $CoFe_2O_4$@TRIS@sulfated boric acid (**b**, **b1**) MNPs
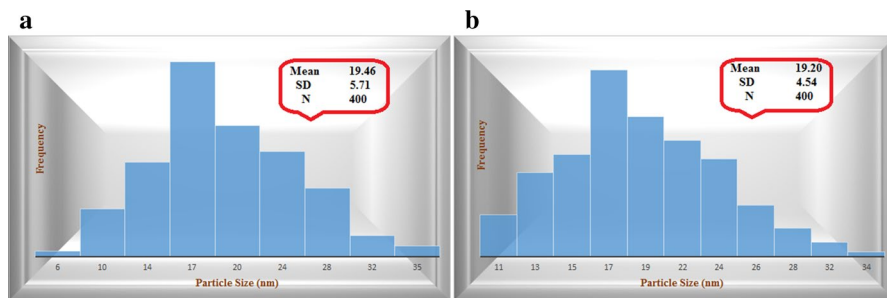

Fig. 3 The size histogram of $CoFe_2O_4$ (**a**) and $CoFe_2O_4$@TRIS@sulfated boric acid (**b**) MNPs
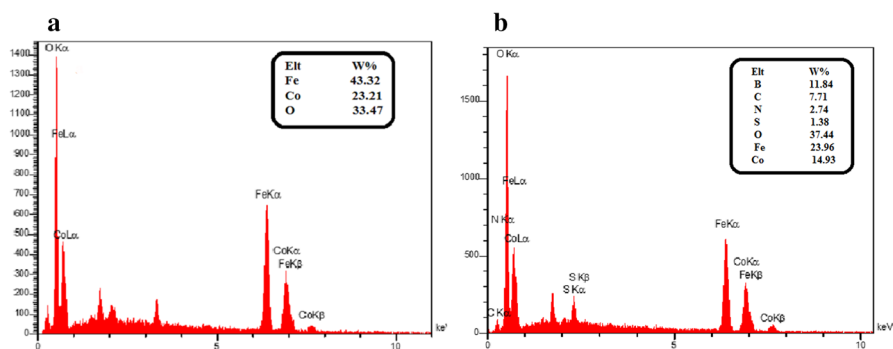
Fig. 4 EDS spectrum of CoFe$_2$O$_4$ (**a**) and CoFe$_2$O$_4$@TRIS@sulfated boric acid (**b**) MNPs
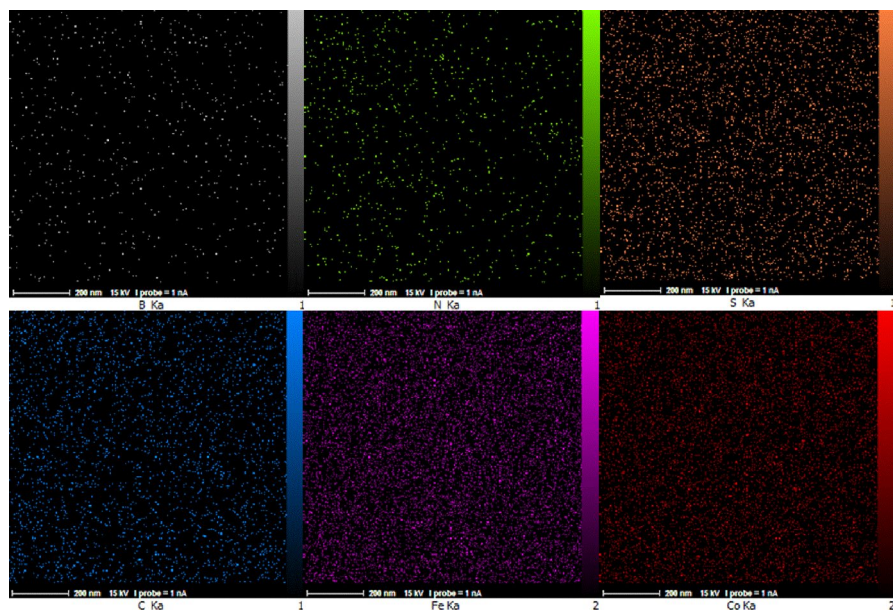

Fig. 5 The X-ray mapping of CoFe$_2$O$_4$@TRIS@sulfated boric acid MNPs

mainly related to the evaporation of the adsorbed solvent and water from the surface of CoFe$_2$O$_4$@TRIS@sulfated boric acid nanoparticles. The second mass loss, in the regions 150–330 °C (about 4.21%), is due to the decomposition of sulfuric acid functional groups (SO$_3$H). According to this mass loss, 42.12 mg (0.52 mmol) of the SO$_3$H group was loaded on 1 g of CoFe$_2$O$_4$ nanoparticles. The final mass loss, at higher 330 °C (5.25%), is attributed to the decomposition of other organic moieties on the surface of CoFe$_2$O$_4$@TRIS@sulfated boric acid nanoparticles, which confirmed the grafting of organic moieties on the surface of CoFe$_2$O$_4$ MNPs. According to these results, 0.26 mmol of the organic layer (TRIS@boric acid) was loaded on 1 g of CoFe$_2$O$_4$ nanoparticles. Moreover, the
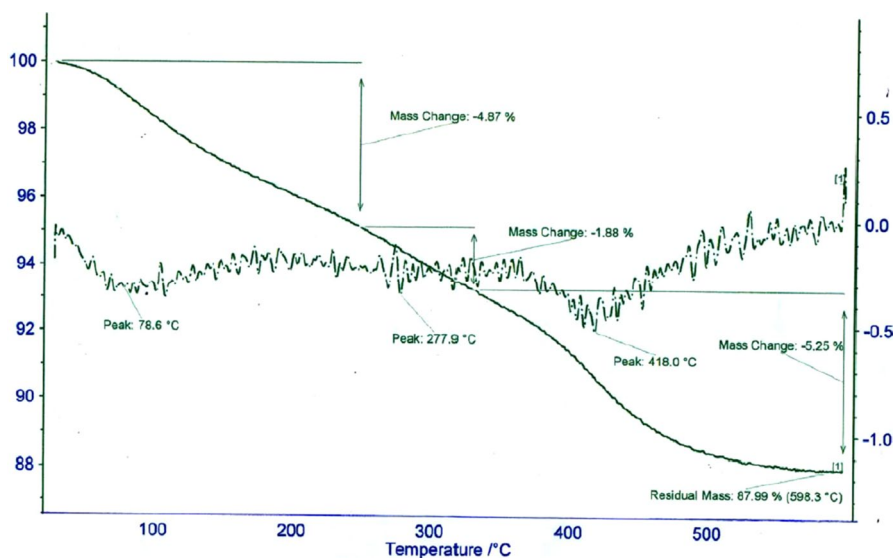
Fig. 6 TGA and DTG curves of CoFe$_2$O$_4$@TRIS@sulfated boric acid MNPs

DTG curve showed that CoFe$_2$O$_4$@TRIS@sulfated boric acid nanoparticles are stable below 277.9 °C.

The XRD patterns of CoFe$_2$O$_4$@TRIS@sulfated boric acid nanoparticles are illustrated in Fig. 7. As depicted in Fig. 7, there were seven diffraction peaks at 62.73°, 57.17°, 53.89°, 43.47°, 35.45°, 30.06°, and 18.23° for CoFe$_2$O$_4$ MNPs that
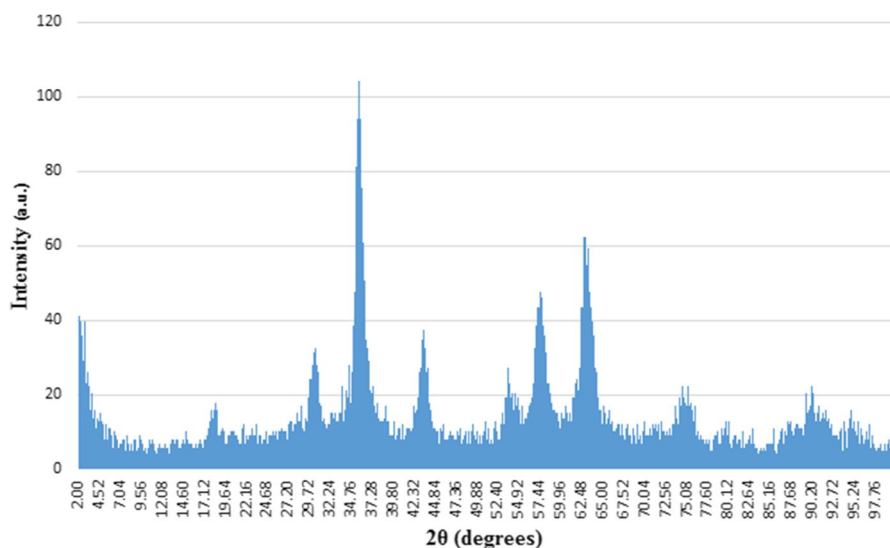

Fig. 7 XRD pattern of CoFe$_2$O$_4$@TRIS@sulfated boric acid MNPs

were indicated by the respective indicators (4 4 0), (5 1 1), (4 2 2), (4 0 0), (3 1 1), (2 2 0), and (1 1 1) (JCPDS Card No. 03–0864). This pattern is in good agreement with the standard $CoFe_2O_4$ XRD pattern [24, 25]. Furthermore, this pattern shows that the structure of cobalt ferrite nanoparticles was maintained after modification with the organic layer (TRIS@sulfated boric acid).

Figure 8 shows the magnetization curves for the $CoFe_2O_4$ (curve **a**) and $CoFe_2O_4$@TRIS@sulfated boric acid (curve **b**) nanoparticles. The saturation magnetization (Ms) values of pure $CoFe_2O_4$ and $CoFe_2O_4$@TRIS@sulfated boric acid nanoparticles are 28.4, and 23.0 emu/g, respectively. Due to immobilization and loading of the organic layer on the surface of cobalt ferrite nanoparticles, the Ms value of $CoFe_2O_4$@TRIS@sulfated boric acid nanoparticles is smaller than that of the $CoFe_2O_4$ nanoparticles. The area of the hysteresis loop for the $CoFe_2O_4$@ TRIS@sulfated boric acid nanoparticles is bigger than for the $CoFe_2O_4$ nanoparticles, so the $CoFe_2O_4$@TRIS@sulfated boric acid nanoparticles are the harder magnetic material with larger coercivity. These materials are difficult to magnetize and demagnetize.

Catalytic study

After the characterization of the new nanocatalyst, its catalytic activity for the synthesis of 2-amino-3-cyanopyridine derivatives was explored (Scheme 1). As can be seen in Table 1, the optimal reaction conditions were investigated on the condensation of 4-chloroacetophenone (1.0 mmol), malononitrile (1.0 mmol), ammonium acetate (1.5 mmol), and 4-chlorobenzaldehyd (1.0 mmol). At first, the model reaction was performed in various solvents such as ethanol, water, and ethanol:water (1:1), as well as solvent-free condition at 70 °C. Results showed that the kind of solvent had a strong effect on yield and time of reaction in the present 0.01 g of $CoFe_2O_4$@TRIS@sulfated boric acid nanoparticles as a heterogeneous catalyst and the best result was obtained in solvent-free condition (Table1, Entry 4). Then, the different amounts of $CoFe_2O_4$@TRIS@sulfated boric acid nanoparticles examined to investigate the effect of them in the model reaction. As can be seen in Table 1, in the absence of $CoFe_2O_4$@TRIS@sulfated
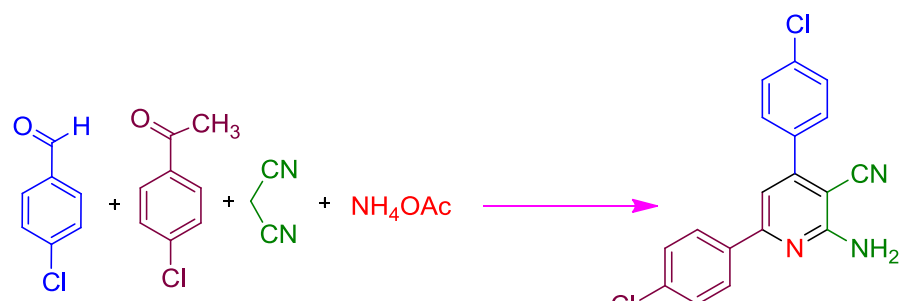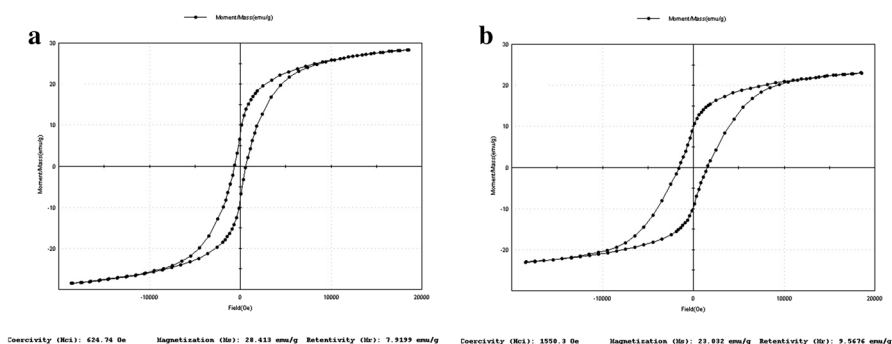

Fig. 8 VSM spectra of $CoFe_2O_4$ (**a**) and $CoFe_2O_4$@TRIS@sulfated boric acid (**b**) MNPs

Table 1 Optimization of reaction conditions for the synthesis of 2-amino-3-cyanopyridines

Entry	Catalyst (g)	Solvent	Temperature (°C)	Time (min)	Yield (%)
1	0.01	EtOH	70	80	46
2	0.01	H$_2$O:EtOH (1:1)	70	85	41
3	0.01	H$_2$O	70	95	34
4	0.01	Solvent free	70	20	54
5	0.005	Solvent free	100	10	80
6	0.01	Solvent free	100	10	62
7	0.015	Solvent free	100	10	64
8	**0.005**	**Solvent free**	**90**	**10**	**82**
9	0.005	Solvent free	120	5	73
10	0.005	Solvent free	80	10	69
11	0.005	Solvent free	70	15	68
12	No catalyst	Solvent free	120	10	45

Bold indicates appropriate reaction condition to produce high amount of product

boric acid nanoparticles, the reaction was performed in the lowest yield and highest time. The best result showed in 0.005 g of CoFe$_2$O$_4$@TRIS@sulfated boric acid nanoparticles (Table 1, Entry 5). Finally, the catalytic activity of CoFe$_2$O$_4$@TRIS@sulfated boric acid nanoparticles was investigated in the different reaction temperatures (from r.t to 120 °C). At the results, the highest yield and the lowest time were obtained in the reaction at 90 °C (Table 1, Entry 8).

On the basis of optimal condition, the efficiency of CoFe$_2$O$_4$@TRIS@sulfated boric acid nanoparticles as a heterogeneous nanocatalyst was evaluated in the synthesis of 2-amino-3-cyanopyridine derivatives with a diverse range of electron-withdrawing and electron-donating aldehydes and the various derivatives of acetophenone. Based on the summarized results in Table 2, all the synthesized products were obtained in the highest yield and the lowest time that confirmed the very high catalytic activity of CoFe$_2$O$_4$@TRIS@sulfated boric acid nanoparticles for the synthesis of 2-amino-3-cyanopyridine derivatives.

Table 2 Synthesis of 2-amino-3-cyanopyridine derivatives in the presence of CoFe$_2$O$_4$@THAM@sulfated boric acid (0.005 g) as catalyst under solvent-free condition at 90 °C

| Entry	R$_1$	R$_2$	Product	Time (min)	Isolated Yield (%)	M.p (°C)	M.p (°C) [Lit.] references
1	4-Cl	4-Cl	**5a**	10	82	277–279	280–282 [26]
2	H	H	**5b**	35	73	184–186	183–185 [27]
3	3.4-diOMe	4-Cl	**5c**	15	89	205–207	207–208 [27]
4	3-NO$_2$	4-Cl	**5d**	10	82	276–278	277–279 [27]
5	4-Cl	H	**5e**	25	80	187–189	186–188 [27]
6	3-NO$_2$	H	**5f**	20	95	196–198	198–200 [27]
7	4-NO$_2$	H	**5g**	15	83	167–170	170–173 [28]
8	4-OMe	4-Cl	**5h**	20	63	203–206	205–207 [29]
9	4-Cl	4-Me	**5i**	15	82	174–176	173–175 [30]
10	4-NO$_2$	4-Me	**5j**	15	77	198–200	201–203 [31]
11	H	4-Me	**5k**	25	67	158–161	160–163 [30]

The proposed mechanism for the synthesis of 2-amino-3-cyanopyridines is shown in Scheme 3. First, CoFe$_2$O$_4$@TRIS@sulfated boric acid nanoparticles as catalyst via protonation of the carbonyl group of aldehydes and ketones generate convenient electrophiles. The Knoevenagel condensation between active aldehydes **1** and malononitrile **3** produces the arylidene malononitrile **A**. In the other hand, active acetophenones **2** reacts with ammonium acetate **4** to give enamine **B**. In the next step, Michael addition of arylidene malononitrile **A** to enamine **B** was formed the intermediate **C**. Finally, corresponding products (**5a–k**) will be generated via subsequent stages intramolecular cyclization/isomerization/aromatization.

Recyclability study

Figure 9 displays the results from reusability tests of CoFe$_2$O$_4$@TRIS@sulfated boric acid nanocatalyst in the model reaction under optimal conditions. For this purpose, the nanocatalyst was magnetically separated from the reaction solution after every cycle and washed several times with ethanol, dried at 60 °C in an oven, and reused in the next cycle. As shown in Fig. 9, the nanocatalyst could be stable for five cycles and reused without any significant loss in its catalytic activity. As a result, the synthesized nanocatalyst has highly recyclability and stability that make it valuable in the organic synthesis.

Comparison

Compared with the reported protocols for the synthesis of the 2-amino-3-cyano-pyridines, as shown in Table 3, the present procedure for the synthesis of 2-amino-3-cyanopyridine derivatives possesses the advantages of high yield of product, short reaction time that affirmed the high catalytic activity of the CoFe$_2$O$_4$@TRIS@
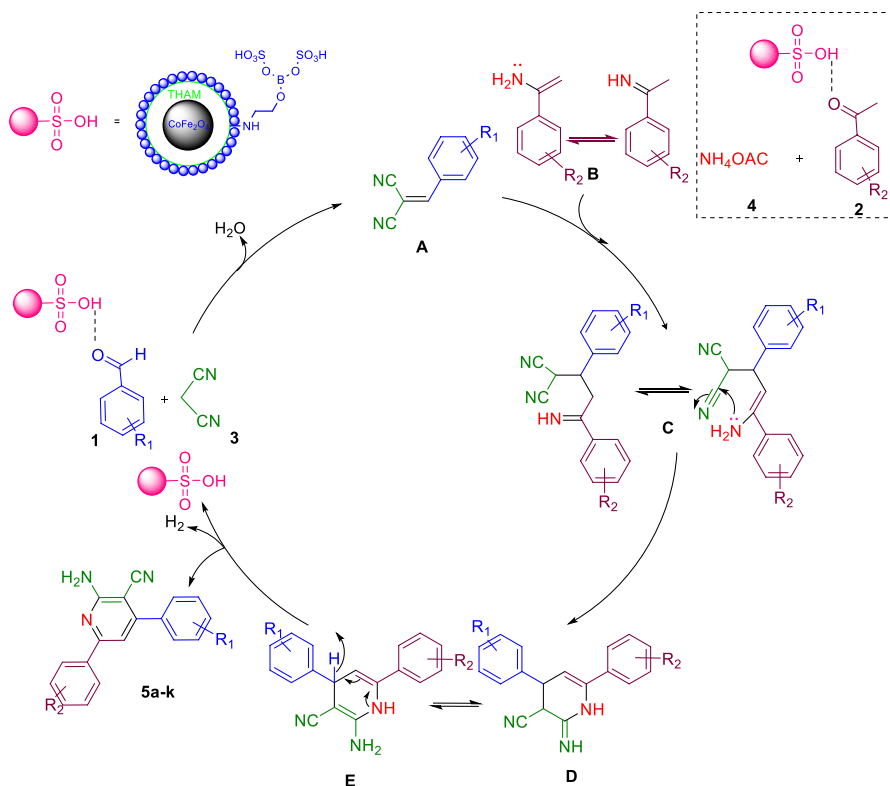
Scheme 3 The proposed mechanism for the synthesis of 2-amino-3-cyanopyridines
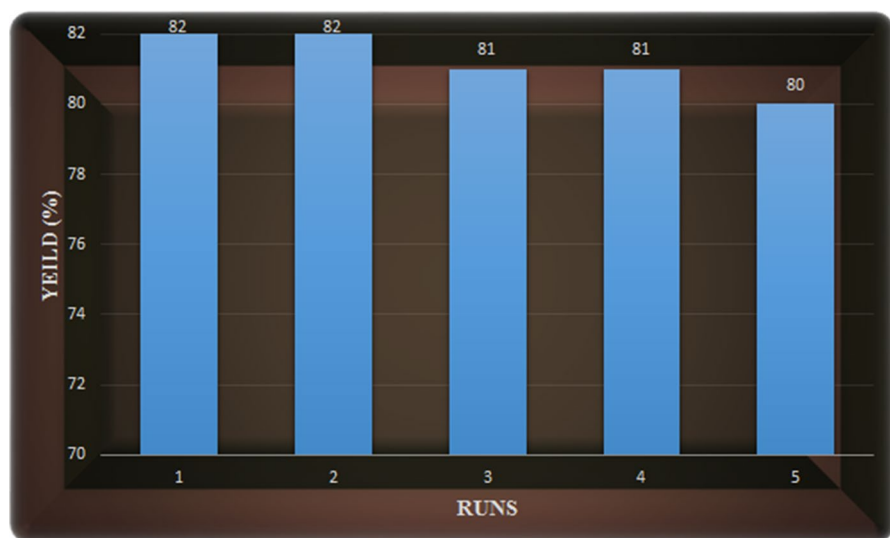

Fig. 9 Reusability tests of CoFe$_2$O$_4$@TRIS@sulfated boric acid nanocatalyst in the synthesis of model reaction (**5a**)

Table 3 Comparison of the efficiency of CoFe$_2$O$_4$@TRIS@sulfated boric acid nanocatalyst with other catalysts in literature

Entry	Catalyst	Amount of catalyst	Condition	Time	Yield (%)	References
1	Nanomagnetic catalyst bearing morpholine tags	(10 mg)	Solvent-free, 80 °C	10–25 min	81–95	[25]
2	Nano-Fe$_3$O$_4$	(30 mg)	Solvent-free, 80 °C	50–80 min	68–91	[31]
3	Yb (PFO)$_3$	(2.5 mol%)	EtOH, reflux	1.5 h	68–93	[32]
4	Iron (III) phosphate	(10 mol%)	ETOH, reflux	2–4.5 h	65–93	[33]
5	PDMAF-MNPs	(40 mg)	EtOH, reflux	1–3.5 h	74–93	[34]
6	Graphene oxide	(10 mol%)	H$_2$O, 80 °C	5 h	75–97	[35]
7	CoFe$_2$O$_4$@TRIS@ sulfated boric acid	(5 mg)	Solvent-free, 90 °C	10–35 min	63–95	This work

sulfated boric acid nanocatalyst as a novel, green, and heterogeneous magnetically reusable nanocatalyst.

Conclusions

In conclusion, this study presents a new and highly proficient CoFe$_2$O$_4$@TRIS@sulfated boric acid nanoparticle catalysed procedure for easy access to 2-amino-3-cyanopyridines from the one-pot four-component reaction between aryl aldehydes, malononitrile, ketones, and ammonium acetate in a green solvent. FT-IR, XRD, MAP, EDS, SEM, VSM, and TG/DTG analysis results can be fully shown immobilization of TRIS@sulfated boric acid onto CoFe$_2$O$_4$ nanostructured. Easy handling of the catalyst, high recyclability, environmental acceptability, and use of commercially available cheap starting materials are the other privilege features of this research.

References

1. A.H. Lu, E.E. Salabas, F. Schüth, Angew. Chem. Int. Ed. **46**, 1222 (2007)
2. C. Bergemann, D. Müller-Schulte, J.A. Oster, L. Brassard, A.S. Lübbe, J. Magn. Magn. Mater. **194**, 45 (1999)
3. S. Mornet, S. Vasseur, F. Grasset, P. Veverka, G. Goglio, A. Demourgues, J. Portier, E. Pollert, E. Duguet, Prog. Solid State Chem. **34**, 237 (2006)

4. C. Pereira, A.M. Pereira, C. Fernandes, M. Rocha, R. Mendes, M.P. Fernández-García, A. Guedes, P.B. Tavares, J.M. Grenèche, J.P. Araújo, C. Freire, Chem. Mater. **24**, 1496 (2012)
5. T. Hyeon, Chem. Commun. **8**, 927 (2003)
6. M. Kazemi, M. Ghobadi, A. Mirzaie, Nanotechnol. Rev. **7**, 43 (2018)
7. F. Saberi, S. Ostovar, R. Behazin, A.R. Rezvani, A. Ebrahimi, H.R. Shaterian, New. J. Chem. **44**, (2020)
8. D. Katheriya, N. Patel, H. Dadhania, A. Dadhania, J. Iran. Chem. Soc. (2020)
9. T. Tamoradi, S.M. Mousavi, M. Mohammadi, New. J. Chem. **44**, 3012–3020 (2020)
10. M. Salimi, F. Esmaeli-nasrabadi, R. Sandaroos, Appl. Organometal. Chem. **35**, e6074 (2020)
11. M. Esmaeilpour, S. Zahmatkesh, N. Fahimi, M. Nosratabadi, Appl. Organometal. Chem. **32**, 4302 (2018)
12. S. Suganuma, K. Nakajima, M. Kitano, D. Yamaguchi, H. Kato, S. Hayashi, M. Hara, Solid State Sci. **12**, 1029 (2010)
13. F. Zhang, Y. Zhao, L. Sun, L. Ding, Y. Gu, P. Gong, Eur. J. Med. Chem. **46**, 3149 (2011)
14. K. Gobis, H. Foks, A. Kędzia, M. Wierzbowska, Z. Zwolska, J. Heterocycl. Chem. **46**, 1271 (2009)
15. A.A. Bekhit, A.M. Baraka, Eur. J. Med. Chem. **40**, 1405 (2005)
16. T. Murata, M. Shimada, S. Sakakibara, T. Yoshino, H. Kadono, T. Masuda, M. Shimazaki, T. Shintani, K. Fuchikami, K. Sakai, H. Inbe, Bioorg. Med. Chem. Lett. **13**, 913 (2003)
17. T. Murata, M. Shimada, H. Kadono, S. Sakakibara, T. Yoshino, T. Masuda, M. Shimazaki, T. Shintani, K. Fuchikami, K.B. Bacon, K.B. Ziegelbauer, Bioorg. Med. Chem. Lett. **14**, 4013 (2004)
18. J. Deng, T. Sanchez, L.Q. Al-Mawsawi, R. Dayam, R.A. Yunes, A. Garofalo, M.B. Bolger, N. Neamati, Bioorg. Med. Chem. **15**, 4985 (2007)
19. M. Mantri, O. De Graaf, J. Van Veldhoven, A. Goblyos, J.K. Von Frijtag Drabbe Kunzel, T. Mulder-Krieger, R. Link, H. De Vries, M.W. Beukers, J. Brussee, A.P. Ijzerman, J. Med. Chem. **51**, 4449 (2008)
20. H. Faroughi Niya, N. Hazeri, M.T. Maghsoodlou, Appl. Organometal. Chem. **34**, 5472 (2020)
21. H. Faroughi Niya, N. Hazeri, M.R. Kahkhaie, M.T. Maghsoodlou, Res. Chem. Intermed. **3**, 1 (2020)
22. M. Fatahpour, F.N. Sadeh, N. Hazeri, M.T. Maghsoodlou, M.S. Hadavi, S. Mahnaei, J. Saudi Chem. Soc. **21**, 998 (2017)
23. H. Faroughi-Niya, N. Hazeri, M. Fatahpour, M.T. Maghsoodlou, Res. Chem. Intermed. **46**, 3651 (2020)
24. F. Yan, S. Zhang, X. Zhang, C. Li, C. Zhu, C. Zhang, Y. Chen, J. Mater. Chem. C **6**, 12781 (2018)
25. F.R. Lamastra, F. Nanni, L. Camilli, R. Matassa, M. Carbone, G. Gusmano, Chem. Eng. J. **162**, 430 (2010)
26. S. Kalhor, M. Yarie, M. Rezaeivala, M.A. Zolfigol, Res. Chem. Intermed. **45**, 3453 (2019)
27. H. Pejman, N. Hazeri, M. Fatahpour, H. Faroughi Niya, Rev. Roum. Chim. **64**, 241 (2019)
28. F. Tamaddon, S.E. Tadayonfar, J. Mol. Struct. **1207**, 127728 (2020)
29. F. Tamaddon, S. Ghazi, M.R. Noorbala, J. Mol. Catal. B Enzym. **127**, 89–92 (2016)
30. G.M. Ziarani, S. Bahar, A. Badiei, J. Iran. Chem. Soc. **16**, 365–372 (2019)
31. M.M. Heravi, S.Y.S. Beheshtiha, M. Dehghani, N. Hosseintash, J. Iran. Chem. Soc. **12**, 2075–2081 (2015)
32. J. Tang, L. Wang, Y. Yao, L. Zhang, W. Wang, Tetrahedron Lett. **52**, 509 (2011)
33. M. Zadpour, F.K. Behbahani, Monatsh. Chem. **146**, 1865 (2015)
34. S. Asadbegi, M.A. Bodaghifard, A. Mobinikhaledi, Res. Chem. Intermed. **46**, 1629 (2020)
35. D. Khalili, Tetrahedron Lett. **57**, 1721 (2016)